Geochemical Perspectives Letters EAG

Zircon as a pathfinder to REE mineralisation

I.W. Hillenbrand[1*]

https://doi.org/10.7185/geochemlet.2540

Abstract

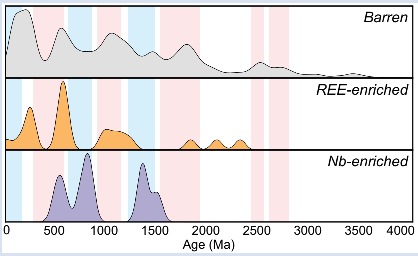

Carbonatites and alkaline silicate rocks are major primary sources of the rare earth elements (REE) and other critical metals, such as Nb. Despite the economic significance of these rocks, their formation and the processes of REE enrichment are poorly understood. Here, statistical analysis of a global dataset demonstrates that zircon geochemistry is a powerful recorder of REE metallogenesis and a potential pathfinder for REE deposits. Zircons from REE and Nb fertile intrusions lack Eu anomalies and have elevated Gd/Yb and Th/Yb, indicating they crystallised from magmas that originated from deep, oxidised and enriched mantle sources. Complexes with Nb enrichment have low U/Nb, reflecting an enriched mantle source, whereas high U/Nb in REE-only fertile intrusions suggest a subduction-metasomatised mantle source. Machine learning models demonstrate high accuracy in classifying zircon from barren and fertile deposits. Classification of detrital zircons shows that REE-enriched deposits correlate with supercontinent assembly, whereas Nb fertile complexes are associated with supercontinent breakup. This approach offers a new, mineral to global scale, petrologic and exploration tool that enhances understanding of REE metallogenesis.

Received 23 April 2025 | Accepted 10 September 2025 | Published 23 October 2025

Introduction

Escalating global demand for rare earth elements (REEs; lanthanides + Y) is driven by their critical role in energy production, national defence and medical technologies (Fortier *et al.*, 2019; Alonso *et al.*, 2023). Current REE supplies are insufficient to meet projected demand, necessitating the discovery of new deposits (Jowitt *et al.*, 2018). Exploration methodologies for REE deposits lag behind those established for other mineral systems that have long been exploited, such as copper (Berger *et al.*, 2009; Champion and Huston, 2016; Ford *et al.*, 2023). Carbonatites and alkaline silicate rocks are the primary hosts for magmatic-derived REE deposits and often contain economic concentrations of other critical commodities, including high field strength elements (HFSEs) like niobium (Nb); yet, these rocks remain poorly understood due to their relative scarcity and susceptibility to alteration (Castor, 2008; Gibson *et al.*, 2024). Understanding the geochemical signatures and petrogenesis of REE-enriched plutons is vital for constructing effective exploration models and elucidating the geodynamic and petrologic processes that govern their formation (Goodenough *et al.*, 2021; Beard *et al.*, 2023).

In this study, I present a statistical analysis of a global compilation of zircon trace element data from barren and REE ± Nb fertile igneous rocks. This synoptic approach aims to identify the distinctive geochemical signatures associated with magmatic REE ± Nb mineralisation, thereby providing critical insights into the formation and economic potential of alkaline-carbonatite complexes. I then explore how machine learning algorithms can leverage multivariate geochemical datasets to identify zircon from fertile intrusions. This approach underscores the efficacy of zircon petrochronology and offers not only a refined understanding of REE metallogenesis but a new exploration tool.

Methods

Data compilation and filtering. Zircon ($ZrSiO_4$) is a widely used mineral geochronometer that preserves a geochemical record of its parental magma composition, which can be retained through high temperature processes, weathering and sediment transport (Grimes *et al.*, 2015; Loucks *et al.*, 2024). Zircon trace element concentrations were compiled from the published literature (all sources and data are provided in the Supplementary Information) and classified into three categories (following Berger *et al.*, 2009; Simandl and Paradis, 2018): (1) *barren*: magmatic zircon from carbonatite, alkaline and calc-alkaline intrusions without REE or Nb enrichment; (2) *Nb ± REE*: magmatic zircon from carbonatite and alkaline intrusions with Nb enrichment, with or without associated REE enrichment; and (3) *REE*: magmatic zircon from carbonatite and alkaline silicate intrusions with REE enrichment but lacking Nb mineralisation (Fig. 1). Only primary magmatic (autocrystic) zircon analyses were retained, excluding altered, recrystallised, hydrothermal or inherited grains as defined in the original studies. In some cases, such as the Mountain Pass intrusive suite, the carbonatite lacks zircon but zircon is present in cogenetic alkaline silicate plutons (Benson *et al.*, 2025). In these cases, zircon from the associated silicate rocks was included in the compilation and assigned to the same class as the deposit. This was done to (1) test if zircon from the alkaline silicate suites retained the signature of the REE-enriched intrusions, and (2) leverage associated zircon-bearing

1. U.S. Geological Survey, Denver, CO 80228
* Corresponding author (email: ihillenbrand@usgs.gov)

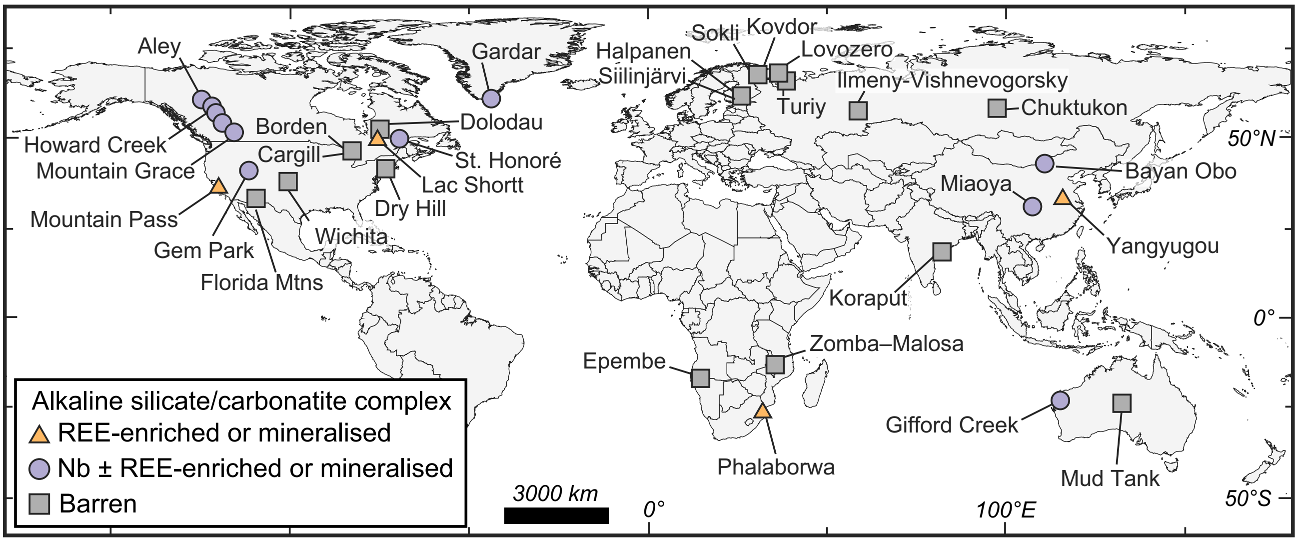

Figure 1 Map showing the present day locations of mineralised and barren alkaline silicate and carbonatite intrusions with zircon trace and rare earth element data. Localities are symbolised by their mineralised or barren classification.

rocks as a tracer for mineralised but zircon-free intrusions. Only autocrystic zircon with <1 ppm La, indicative of contamination by LREE-rich phases, such as apatite (Loucks *et al.*, 2024), and <20 % discordance or <10 % reverse discordance, indicative of open-system behaviour, were retained. The filtered dataset includes 2153 zircon analyses, with 253 from carbonatites, 962 from alkaline silicate rocks and 938 from calc-alkaline plutons. Collectively, 1851 zircons are from barren intrusions, 113 are from REE fertile complexes, and 189 are from Nb ± REE-enriched rocks.

Data treatment and pre-processing. Only complete suites of elements were included as missing values can lead to information loss that reduces the accuracy of the models. Elemental concentrations retained in the analysis are U, Th, Nb, Ce, Pr, Nd, Sm, Eu, Gd, Dy, Er, Yb, Lu and Hf, as they were available for all mineralised intrusions. Several key parameters were also considered: Eu anomaly (Eu/Eu*; $Eu_N/(Sm_N{*}Gd_N)^{0.5}$), the sum of the heavy rare earth elements (∑HREE, Gd–Lu), Lu/Hf, Th/U, Dy/Yb, U/Nb, U/Yb, Th/Nb, Sm/Yb, Th/Yb, Ce/U and Gd/Yb. Comparison of ratios, rather than absolutes concentrations, minimises compositional variations due to elemental partitioning at different zircon crystallisation temperatures (Grimes *et al.*, 2015). All values were given equal weighting to prevent any single feature from biasing the analysis.

Machine learning. Machine learning uses computational algorithms to recognise trends and classify samples based on learned patterns from large multivariate datasets. The scikit-learn package was used to implement six common algorithms briefly summarised here (see Supplementary Information for complete details). (1) *Naïve Bayes*: a probabilistic classifier that predicts class membership based on Bayes' theorem, assuming feature independence. (2) *Decision tree:* represents decisions as a branching tree structure, where each branch corresponds to a feature-based decision. (3) *Random forest:* combines multiple decision trees to improve prediction accuracy and reduce overfitting, which can enhance model robustness. (4) *Support vector machines*: finds optimal hyperplanes to separate data classes. (5) *k-nearest neighbours*: classifies samples based on the majority class of their nearest neighbours in the feature space. (6) *Gradient boosting*: iteratively builds predictive models by sequentially correcting the errors of previous trees.

Each model was trained using 80 % of the compilation with 20 % of the data reserved for validation and testing. This comparative approach aimed to evaluate the efficacy of each algorithm to identify the most robust and reliable model(s) for interpreting the data, and to mitigate potential biases associated with any single method. Feature importance analysis was conducted to validate and improve the interpretability of the decision tree, random forest and gradient boosting models by evaluating which variables most influence the models.

Results

Machine learning classification models achieved overall accuracies of 86 % to 97 % (Fig. 2a; Table S-1). The Naïve Bayes model exhibited the lowest performance with the lowest overall accuracy (86 %) and the poorest precision for both the REE-only (31 %) and Nb ± REE groups (64 %). Random forest, support vector machines and *k*-nearest neighbours demonstrated the highest accuracies (97 %). Decision tree and gradient boosting models achieved slightly lower accuracies (95–96 %). All models except Naïve Bayes yielded F1-scores of 81 to 99 (Table S-2).

Feature importance analysis across the decision tree, random forest and gradient boosting models revealed consistent patterns in identifying key geochemical discriminators. The most important features for zircon classification are Eu/Eu*, U/Nb, Nb/Yb, Ce/U, Th/Yb and U/Yb (Fig. 2b). The decision tree and gradient boosting models show closer agreement in their feature importance rankings, whereas the random forest model diverges slightly with respect to the relative importance of Ce/U and Th/Yb.

Discussion

Model evaluation. The tree- and kernel-based models (decision tree, random forest, support vector machines, *k*-nearest neighbours and gradient boosting) demonstrated robust and balanced classification across all classes. The lower performance of Naïve Bayes shows its assumption of independent predictor variables may not be met in geochemical datasets due to shared petrogenetic processes. The success of the tree- and kernel-based models highlights these algorithms' ability to capture the complexity

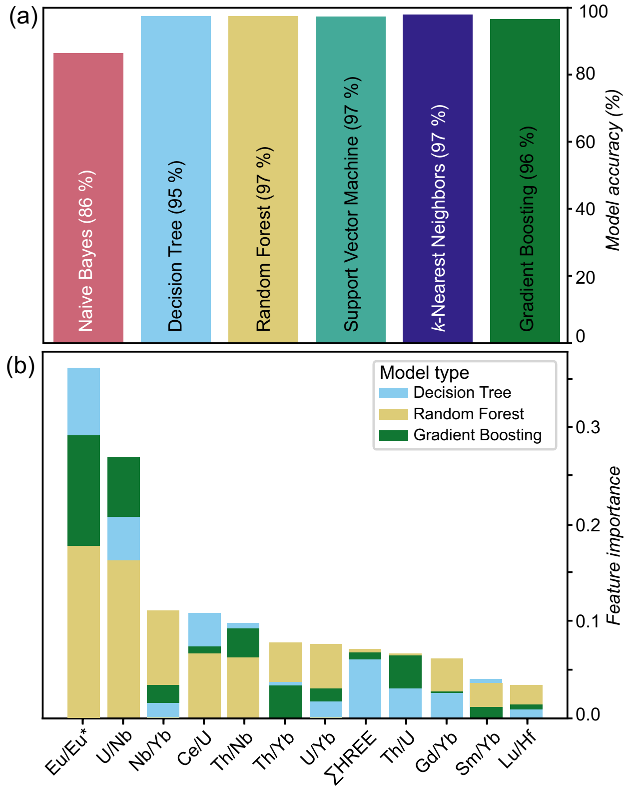

Figure 2 Bar charts showing the **(a)** accuracy of each machine learning algorithm and **(b)** feature importance calculations for the tree-based classification methods.

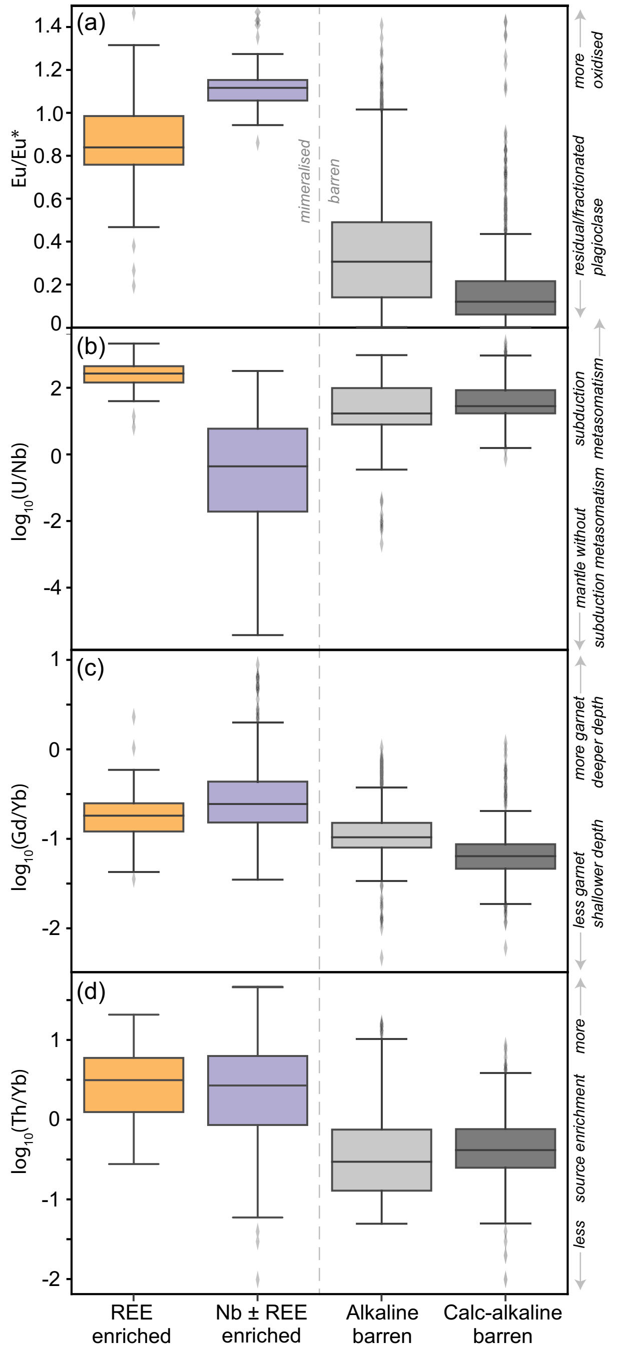

Figure 3 Box and whisker plots showing the distribution of **(a)** Eu anomaly (Eu/Eu*), **(b)** U/Nb, **(c)** Gd/Yb and **(d)** Th/Yb in zircon from fertile and barren intrusions. The alkaline barren category includes both carbonatite and alkaline silicate rocks.

in multivariate geochemical systems, which may not be readily apparent or fully resolved through conventional geochemical discrimination approaches.

Despite the overall strong classification performance, some limitations must be considered. The class imbalance, specifically the lesser amount of analyses from fertile intrusions compared to barren samples, could influence model performance (Ghosh *et al.*, 2024). Some complexes also contain larger numbers of samples and zircon analyses, while others are less well characterised. The compiled data were collected over the past 20 years using different labs, instruments (*e.g.*, laser ablation inductively coupled plasma mass spectrometry (LA-ICP-MS) *vs.* secondary ion mass spectrometry (SIMS) and other procedures; *cf.* Horstwood *et al.*, 2016). Although it is assumed that the published data are broadly comparable, the dataset could be limited by methodological differences, particularly for challenging measurements, such as Nb. The age ranges for fertile (2.6–0.3 Ga) and barren alkaline-carbonatite complexes (2.6–0.1 Ga) in the training dataset are limited. Archean geochemical processes, thermal gradients and tectonic regimes may have been distinct from those represented in the training data (Condie, 2021), and careful consideration is warranted when extrapolating these classification models to older zircons (Triantafyllou *et al.*, 2023).

Geochemical signatures and genesis of REE-enriched intrusions. Feature importance analysis (Fig. 2b) identified key zircon geochemical signatures—Eu/Eu*, U/Nb, Gd/Yb and Th/Yb—that effectively discriminate between fertile and barren deposits (Fig. 3) regardless of source rock type (calc-alkaline silicate, alkaline silicate, carbonatite). REE and Nb ± REE-enriched intrusions display minimal to slightly positive median Eu/Eu* (0.8–1.1; Fig. 3a). In contrast, zircons from barren intrusions typically exhibit negative Eu/Eu* anomalies (median: 0.1–0.3). Zircon Eu/Eu* is influenced by plagioclase stability and magma oxidation state (Trail *et al.*, 2012), as well as by temperature, water content and source composition. As carbonatite and alkaline rocks are mantle-derived, the lack of significant Eu/Eu* anomalies in the REE fertile intrusions suggests derivation from a deep, plagioclase-free and oxidised source. This supports the work of Braunger *et al.* (2020) who showed that carbonatites and REE deposits crystallise from oxidised mantle-derived melts.

Figure 3b shows that zircons from Nb ± REE deposits have lower median U/Nb ratios (0.41) compared to REE-only deposits (302). Zircon U/Nb from barren alkaline (17) and calc-alkaline (30) are intermediate. Zircon from undepleted to enriched mantle sources commonly yield U/Nb less than 20, while U/Nb greater than 30 reflects a subduction-modified source (Grimes *et al.*, 2015). The low U/Nb ratios in zircon from Nb ± REE deposits may reflect a mantle source region that is enriched in Nb relative to U and lacks the Nb depletion associated with subduction-related metasomatism. This supports the common association of Nb ± REE deposits with rift and intraplate settings with ocean island basalt-like compositions (Gibson *et al.*, 2024). In contrast, high zircon U/Nb in REE-only deposits suggest derivation from a mantle source region that was previously enriched by subduction-related metasomatism (Nadeau *et al.*, 2014; Goodenough *et al.*, 2021; Benson *et al.*, 2025). The mineral data support a broader trend evident from whole-rock data. Goodenough *et al.* (2021) observed that REE-enriched alkaline rocks and carbonatites without Nb enrichment form by melting of a parental lithospheric mantle source that was metasomatised by fluids or melts derived from crustal materials in a subducting slab. Hence, source composition and mantle enrichment processes have an important control on mineralisation type and potential, likely influenced by tectonic processes. Palaeotectonic analysis suggests that REE-enriched complexes are common in syn- to post-collisional environments, where thermal relaxation and decompression cause melting of a source enriched by prior subduction-related metasomatism (Veevers, 2007; Nadeau *et al.*, 2014; Beard *et al.*, 2023; Benson *et al.*, 2025), whereas Nb ± REE complexes are typically associated with rifts and mantle plumes (Goodenough *et al.*, 2021; Gibson *et al.*, 2024). In some cases, rift-related processes can cause melting of subduction-metasomatised mantle hundreds of millions of years after enrichment (Goodenough *et al.*, 2021). Overall, zircon U/Nb (and Nb/Yb) appears to be a key index not only for differentiating REE and Nb fertility in alkaline-carbonatite complexes but also source composition and, to some extent, tectonic setting.

REE- and Nb-enriched plutons exhibit higher median zircon Gd/Yb ratios (0.19–0.24) compared to barren calc-alkaline (0.06) and carbonatite-alkaline intrusions (0.10). Zircon Gd/Yb is largely controlled by the modal abundance of garnet in the source region in mantle-derived rocks, and the elevated Gd/Yb ratios suggest melting at garnet-stable pressures. Melt generation at high pressures yields higher concentrations of REEs, Nb, P and CO_2 for a given mantle source composition (Beard *et al.*, 2023). Both fertile groups show zircon Th/Yb (median: 2.7–3.2) that is elevated above barren intrusions (median: 0.30–0.42). Elevated zircon Th/Yb suggests that mineralised intrusions are derived from source regions that are more enriched in incompatible elements and/or lower degrees of mantle melting (Pearce, 2008; Grimes *et al.*, 2015).

Zircon commonly records the compositions of the magmas from which it crystallised because of its resistance to alteration and diffusion (Loucks *et al.*, 2024). Therefore, it can document the composition of REE ± Nb-enriched *vs.* barren melts and the petrogenetic processes involved in forming magmatic-derived REE deposits. REE ± Nb-enriched intrusions are derived from mantle source regions that are more oxidised, incompatible element-enriched and generated at greater depths than barren intrusions. Alkaline-silicate-carbonatite complexes enriched in Nb have lower U/Nb and higher Nb/Yb, suggesting derivation from ocean island basalt-like mantle source regions that are less influenced by subduction-related processes (Pearce, 2008; Grimes *et al.*, 2015). Elevated zircon U/Nb and lower Nb/Yb in REE-only intrusions suggest derivation from lithospheric mantle sources affected by prior subduction-related metasomatism.

Application to detrital zircon. Detrital zircon petrochronology is used to reconstruct tectonic histories, constrain crustal evolution and identify mineralisation (Condie and Aster, 2010; Nardi *et al.*, 2013; Drabon *et al.*, 2024). Zircon is refractory in sedimentary systems and detrital grains can be used for fertility evaluation and as a tracer of undiscovered deposits. Zircon is well suited as a prospecting vector given its resilience in sedimentary systems, relative ease of isolation from soil and sediment samples and reasonably straightforward and rapid U-Pb and trace element analysis. New classification models for detecting REE and Nb mineralisation in the sedimentary record were tested using a compilation of detrital zircon ages and geochemistry, spanning modern river sediments to Archean sedimentary rocks (Roberts *et al.*, 2024). This dataset was filtered for concordance and inclusions following the methods described in Section 2. Approximately 27,000 zircon grains passed these filters and were classified. All models except the less precise Naive Bayes model yielded similar peaks and distributions. For simplicity, this discussion focuses on the random forest model as it yielded high F1-scores, precision and recall across classes.

More than 99.8 % of the detrital zircons were classified as having barren sources (Fig. 4a), consistent with the rarity of REE and Nb fertile intrusions in the geologic record and the generally low to absent zircon content of carbonatites and alkaline rocks (Beard *et al.*, 2023). Zircon grains classified as being derived from REE-enriched intrusions exhibit age peaks at 2305, 2080, 1820, 1100, 995, 580 and 240 Ma (Fig. 4b), which broadly correspond with the tenures of Nuna (Columbia), Rodinia, Gondwana and Pangea (Pangaea) (Veevers, 2007; Mitchell *et al.*, 2021). Conversely, zircons classified as Nb ± REE-enriched have peaks at 1400, 1350, 800 and 530 Ma, which fall during periods of supercontinent breakup (Fig. 4c). The 530 Ma peak overlaps the timing of post-collisional extension in Gondwana and the opening of the Iapetus Ocean (Veevers, 2007; Néron *et al.*, 2018).

The differences in age distributions between REE and Nb ± REE can inform the linkages between metallogenesis and tectonics. Temporal linkages between supercontinent assembly and REE-only deposits, along with their geochemical characteristics (Section 4.2; Goodenough *et al.*, 2021; Benson *et al.*, 2025), are consistent with REE-only type complexes forming largely in collisional settings (Goodenough *et al.*, 2021; Nadeau *et al.*, 2014; Benson *et al.*, 2025). Nb-enriched complexes correlate temporally with supercontinent breakup, compatible with their

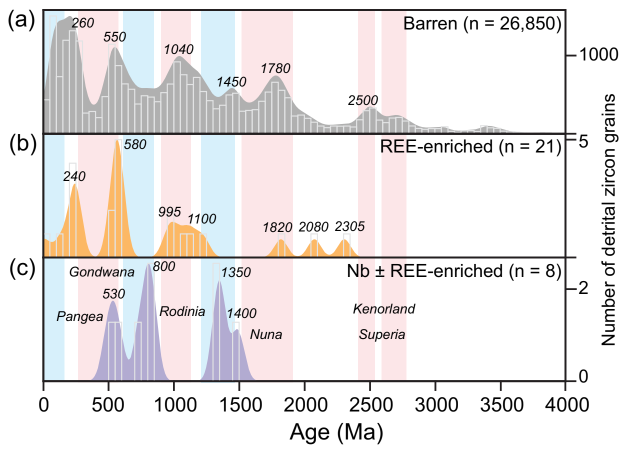

Figure 4 Classification of detrital zircon samples. Kernel density estimates and histograms (50 Myr bandwidth) of detrital zircon classified as being derived from **(a)** barren rocks, **(b)** REE-only deposits and **(c)** Nb ± REE deposits. Red and blue bars represent the timing of supercontinent/supercraton assembly and breakup, respectively (Cawood *et al.*, 2013; Condie, 2021).

formation from enriched mantle sources in rift or intraplate settings (Beard *et al.*, 2023; Gibson *et al.*, 2024).

This application highlights how the machine learning models can classify zircon with geologically reasonable results. While the absolute peaks and relative abundances can be affected by sampling bias, limited data availability, the lower preservation potential of syn-sedimentary magmatic rocks and zircon in rift-related settings (Cawood *et al.*, 2012), and secular changes in petrogenetic process (Triantafyllou *et al.*, 2023), I demonstrate the viability and potential of this approach for constraining the timing, flux and geodynamic processes of REE- and Nb-enriched magmatism.

Implications and Future Directions

Zircon geochemistry effectively discriminates between REE and/or Nb fertile and barren intrusions and is therefore a successful petrogenetic marker for these magmatic-derived deposits. Magmatic REE deposits originate from low degree partial melting of deep, oxidised mantle sources enriched in incompatible elements. The relative enrichment of REE and Nb may be linked to whether the mantle source was previously affected by subduction-related metasomatism. This analysis can be used to assess the mineralisation potential of prospective complexes by comparing their zircon signatures to those of known systems. In provenance studies, the zircon geochemical fingerprint of REE and Nb deposits can be used as a source-to-sink tool or as a mineral "pathfinder" to discover zircon-bearing deposits. Data from more mineralised and barren intrusions, hydrothermal zircons and a broader suite of trace elements (*e.g.*, Ti, Ta, Sc, P), isotopes (*e.g.*, O, Hf) and intensive parameters (*e.g.*, fO_2, temperature) can aid in identifying global to deposit-specific fingerprints and more precise targeting of ore deposits.

Acknowledgements

This research was funded by the U.S. Geological Survey Mineral Resources Program. Any use of trade, firm or product names is for descriptive purposes only and does not imply endorsement by the U.S. Government. I appreciate helpful feedback from Erin Benson, Amy Gilmer, Ben Magnin and Kathryn Watts. Constructive comment from two anonymous reviewers, Carl Beno, Natalie Latysh, and editor Helen Williams are greatly appreciated.

Editor: Helen Williams

Additional Information

Supplementary Information accompanies this letter at https://www.geochemicalperspectivesletters.org/article2540.

Cite this letter as: Hillenbrand, I.W. (2025) Zircon as a pathfinder to REE mineralisation. *Geochem. Persp. Let.* 37, 18–23. https://doi.org/10.7185/geochemlet.2540

References

Alonso, E., Pineault, D.G., Gambogi, J., Nassar, N.T. (2023) Mapping first to final uses for rare earth elements, globally and in the United States. *Journal of Industrial Ecology* 27, 312–322. https://doi.org/10.1111/jiec.13354

Beard, C.D., Goodenough, K.M., Borst, A.M., Wall, F., Siegfried, P.R. *et al.* (2023) Alkaline-Silicate REE-HFSE Systems. *Economic Geology* 118, 177–208. https://doi.org/10.5382/econgeo.4956

Benson, E.K., Watts, K.E., Hillenbrand, I.W. (2025) Geochemistry and radiogenic isotopes constrain the mantle source region of the Mountain Pass Intrusive Suite, California. *Lithos* 508–509, 108060. https://doi.org/10.1016/j.lithos.2025.108060

Berger, V.I., Singer, D.A., Orris, G.J. (2009) Carbonatites of the world, explored deposits of Nb and REE— Database and grade and tonnage models. *U.S. Geological Survey Open-File Report* 2009-1139. https://doi.org/10.3133/ofr20091139

Braunger, S., Marks, M.A.W., Wenzel, T., Chmyz, L., Azzone, R.G., Markl, G. (2020) Do carbonatites and alkaline rocks reflect variable redox conditions in their upper mantle source? *Earth and Planetary Science Letters* 533, 116041. https://doi.org/10.1016/j.epsl.2019.116041

Castor, S.B. (2008) Rare Earth Deposits of North America. *Resource Geology* 58, 337–347. https://doi.org/10.1111/j.1751-3928.2008.00068.x

Cawood, P.A., Hawkesworth, C.J., Dhuime, B. (2012) Detrital zircon record and tectonic setting. *Geology* 40, 875–878. https://doi.org/10.1130/G32945.1

Cawood, P.A., Hawkesworth, C.J., Dhuime, B. (2013) The continental record and the generation of continental crust. *GSA Bulletin* 125, 14–32. https://doi.org/10.1130/B30722.1

Champion, D.C., Huston, D.L. (2016) Radiogenic isotopes, ore deposits and metallogenic terranes: Novel approaches based on regional isotopic maps and the mineral systems concept. *Ore Geology Reviews* 76, 229–256. https://doi.org/10.1016/j.oregeorev.2015.09.025

Condie, K.C. (2021) Two Major Transitions in Earth History: Evidence of Two Lithospheric Strength Thresholds. *The Journal of Geology* 129, 455–473. https://doi.org/10.1086/711141

Condie, K.C., Aster, R.C. (2010) Episodic zircon age spectra of orogenic granitoids: The supercontinent connection and continental growth. *Precambrian Research* 180, 227–236. https://doi.org/10.1016/j.precamres.2010.03.008

Drabon, N., Kirkpatrick, H.M., Byerly, G.R., Wooden, J.L. (2024) Trace elements in zircon record changing magmatic processes and the multi-stage build-up of Archean proto-continental crust. *Geochimica et Cosmochimica Acta* 373, 136–150. https://doi.org/10.1016/j.gca.2024.03.014

Ford, A., Huston, D., Cloutier, J., Doublier, M., Schofield, A., Cheng, Y., Beyer, E. (2023) A national-scale mineral potential assessment for carbonatite-related rare earth element mineral systems in Australia. *Ore Geology Reviews* 161, 105658. https://doi.org/10.1016/j.oregeorev.2023.105658

Fortier, S.M., Hammarstrom, J.M., Ryker, S.J., Day, W.C., Seal II, R.R. (2019) USGS critical minerals review. *Mining Engineering* 71, 35–47. https://pubs.usgs.gov/publication/70206338

Ghosh, K., Bellinger, C., Corizzo, R., Branco, P., Krawczyk, B., Japkowicz, N. (2024) The class imbalance problem in deep learning. *Machine Learning* 113, 4845–4901. https://doi.org/10.1007/s10994-022-06268-8

Gibson, S., McKenzie, D., Lebedev, S. (2024) The distribution and generation of carbonatites. *Geology* 52, 667–671. https://doi.org/10.1130/G52141.1

Goodenough, K.M., Deady, E.A., Beard, C.D., Broom-Fendley, S., Elliott, H.A.L., van den Berg, F., Öztürk, H. (2021) Carbonatites and Alkaline Igneous Rocks in Post-Collisional Settings: Storehouses of Rare Earth Elements. *Journal of Earth Science* 32, 1332–1358. https://doi.org/10.1007/s12583-021-1500-5

Grimes, C.B., Wooden, J.L., Cheadle, M.J., John, B.E. (2015) "Fingerprinting" tectono-magmatic provenance using trace elements in igneous zircon. *Contributions to Mineralogy and Petrology* 170, 46. https://doi.org/10.1007/s00410-015-1199-3

Horstwood, M.S.A., Košler, J., Gehrels, G., Jackson, S.E., McLean, N.M. *et al.* (2016) Community-Derived Standards for LA-ICP-MS U-(Th-)Pb Geochronology – Uncertainty Propagation, Age Interpretation and Data Reporting. *Geostandards and Geoanalytical Research* 40, 311–332. https://doi.org/10.1111/j.1751-908X.2016.00379.x

Jowitt, S.M., Mudd, G.M., Werner, T.T., Weng, Z., Barkoff, D.W., McCaffrey, D. (2018) The Critical Metals: An Overview and Opportunities and Concerns for the Future. In: Arribas R., A.M., Mauk, J.L. (Eds.) *Metals, Minerals, and Society*. Society of Economic Geologists, Littleton, 25–38. https://doi.org/10.5382/SP.21.02

Loucks, R.R., Henríquez, G.J., Fiorentini, M.L. (2024) Zircon and Whole-Rock Trace Element Indicators of Magmatic Hydration State and Oxidation State

Discriminate Copper Ore-Forming from Barren Arc Magmas. *Economic Geology* 119, 511–523. https://doi.org/10.5382/econgeo.5071

Mitchell, R.N., Zhang, N., Salminen, J., Liu, Y., Spencer, C.J., Steinberger, B., Murphy, J.B., Li, Z.-X. (2021) The supercontinent cycle. *Nature Reviews Earth & Environment* 2, 358–374. https://doi.org/10.1038/s43017-021-00160-0

Nadeau, O., Stevenson, R., Jébrak, M. (2014) The Archean magmatic-hydrothermal system of Lac Shortt (Au-REE), Abitibi, Canada: Insights from carbonate fingerprinting. *Chemical Geology* 387, 144–156. https://doi.org/10.1016/j.chemgeo.2014.08.021

Nardi, L.V.S., Formoso, M.L.L., Müller, I.F., Fontana, E., Jarvis, K., Lamarão, C. (2013) Zircon/rock partition coefficients of REEs, Y, Th, U, Nb, and Ta in granitic rocks: Uses for provenance and mineral exploration purposes. *Chemical Geology* 335, 1–7. https://doi.org/10.1016/j.chemgeo.2012.10.043

Néron, A., Bédard, L.P., Gaboury, D. (2018) The Saint-Honoré Carbonatite REE Zone, Québec, Canada: Combined Magmatic and Hydrothermal Processes. *Minerals* 8, 397. https://doi.org/10.3390/min8090397

Pearce, J.A. (2008) Geochemical fingerprinting of oceanic basalts with applications to ophiolite classification and the search for Archean oceanic crust. *Lithos* 100, 14–48. https://doi.org/10.1016/j.lithos.2007.06.016

Roberts, N.M.W., Spencer, C.J., Puetz, S., Keller, C.B., Tapster, S. (2024) Regional trends and petrologic factors inhibit global interpretations of zircon trace element compositions. *Geoscience Frontiers* 15, 101852. https://doi.org/10.1016/j.gsf.2024.101852

Simandl, G.J., Paradis, S. (2018) Carbonatites: Related ore deposits, resources, footprint, and exploration methods. *Applied Earth Science* 127, 123–152. https://doi.org/10.1080/25726838.2018.1516935

Trail, D., Watson, E.B., Tailby, N.D. (2012) Ce and Eu anomalies in zircon as proxies for the oxidation state of magmas. *Geochimica et Cosmochimica Acta* 97, 70–87. https://doi.org/10.1016/j.gca.2012.08.032

Triantafyllou, A., Ducea, M.N., Jepson, G., Hernández-Montenegro, J.D., Bisch, A., Ganne, J. (2023) Europium anomalies in detrital zircons record major transitions in Earth geodynamics at 2.5 Ga and 0.9 Ga. *Geology* 51, 141–145. https://doi.org/10.1130/G50720.1

Veevers, J.J. (2007) Pan-Gondwanaland post-collisional extension marked by 650–500 Ma alkaline rocks and carbonatites and related detrital zircons: A review. *Earth-Science Reviews* 83, 1–47. https://doi.org/10.1016/j.earscirev.2007.03.001